REPORT

Calcium Transduces Plasma Membrane Receptor Signals to Produce Diacylglycerol at Golgi Membranes[*]

Maya T. Kunkel and Alexandra C. Newton[1]

From the Department of Pharmacology, University of California at San Diego, La Jolla, California 92093

Protein kinase C and protein kinase D are potently activated by agonist-evoked increases in diacylglycerol. Using live cell-imaging probes for kinase activity, we have shown that both kinases are robustly activated at the Golgi following stimulation of G_q-coupled receptor signaling pathways, displaying activation signatures at the Golgi that are distinct from those at the plasma membrane. Here we report that Ca^{2+} is the mediator that allows signals received at the plasma membrane to activate these two protein kinases at the Golgi. Specifically, using fluorescence resonance energy transfer-based reporters to image diacylglycerol production, we show that Ca^{2+} is necessary and sufficient to elevate diacylglycerol levels at the Golgi. First, raising intracellular Ca^{2+} by treating cells with thapsigargin induces diacylglycerol production at the Golgi. Second, chelation of intracellular Ca^{2+} prevents UTP-stimulated increases in diacylglycerol at the Golgi. Thus, agonist-evoked increases in intracellular Ca^{2+} cause increases in Golgi diacylglycerol, allowing this intracellular membrane to serve as a platform for signaling by protein kinases C and D.

Diacylglycerol (DAG)[2] is a ubiquitous lipid second messenger generated following activation of numerous G-protein-coupled receptor (GPCR) and tyrosine kinase receptors. The targets of DAG are proteins containing a C1 domain, a membrane-targeting module that binds DAG, thus tethering the parent protein to membranes. Protein kinase C (PKC) family members were the first described targets for DAG; however, at least five distinct DAG-binding families, each depending on C1 domains to recognize DAG, have now been identified, including the protein kinase D (PKD) family (1–3).

Previously, our laboratory designed genetically encoded activity reporters to monitor real-time kinase signaling by PKC and PKD (4, 5). By poising these activity reporters at Golgi membranes, we observed pronounced activity from both PKC and PKD at this intracellular region (Ref. 6 and data not shown). Indeed, the role of PKD at the Golgi in the regulation of Golgi fission and protein transport has been extensively characterized (7, 8). Our reporters revealed pronounced differences in the rate, amplitude, and duration of PKC signaling at the Golgi as compared with plasma membrane. Notably, there is a rapid and transient increase in kinase activity at plasma membrane following G_q-coupled GPCR activation, whereas the activity at Golgi membranes increases more slowly and is sustained (6). The differences in kinetics of these two responses arise from the differences in the production rate and persistence of DAG at Golgi membrane as compared with plasma membrane (6).

DAG levels at Golgi membranes are basally elevated as compared with other intracellular membranes, resulting in the pretargeting of PKD as well as its upstream kinase, PKCδ (9–11). However, an additional agonist-evoked increase in DAG at this location is necessary to activate these two enzymes (6). Although the source of Golgi DAG under basal conditions has been attributed to phosphatidic acid phosphatase (PAP) and sphingomyelin synthase (SMS) (12, 13), the mechanism by which Golgi DAG levels increase following activation of plasma membrane receptors remains to be elucidated.

Here we examine the mechanism of DAG production at Golgi membranes using a genetically encoded, Golgi-targeted, fluorescence resonance energy transfer (FRET) reporter system. We demonstrate that Ca^{2+} is both necessary and sufficient to increase Golgi-localized DAG levels downstream of GPCR signaling from the plasma membrane. Furthermore, through use of a distinct, FRET-based kinase activity reporter, we demonstrate that this Ca^{2+}-mediated pathway is critical for PKD activity at Golgi membranes. Thus, these data identify Ca^{2+} as the key second messenger that controls Golgi-localized production of DAG downstream of GPCRs and, in turn, the function of C1 domain-containing proteins such as PKC and PKD.

EXPERIMENTAL PROCEDURES

Materials—Phorbol 12,13-dibutyrate (PDBu), edelfosine, thapsigargin, propranolol, and UTP were obtained from Calbiochem. 1,2-bis(*o*-Aminophenoxy)ethane-*N,N,N′,N′*-tetraacetic acid tetra(acetoxymethyl) ester (BAPTA-AM) and EGTA were obtained from Sigma.

Plasmid Constructs—MyrPalm-CFP has been previously described (4). YFP-C1b-Y123W was described in Dries *et al.* (11). Golgi-CFP was originally described in Gallegos *et al.* (6). YFP-PKD1 was generated through an N-terminal fusion of YFP to PKD1. Golgi-DKAR was generated by fusing sequences encoding the N-terminal 33 amino acids of endothelial nitric-oxide synthase (eNOS) (14) to DKAR (5).

Cell Culture and Transfection—COS-7 cells were maintained in Dulbecco's modified Eagle's medium containing 5% fetal bovine serum and 1% penicillin/streptomycin at 37 °C in 5% CO_2. Cells were plated onto sterilized glass coverslips in 35-mm dishes prior to transfection. Transient transfection of 1 µg of

[2] The abbreviations used are: DAG, diacylglycerol; PKD, protein kinase D; PKC, protein kinase C; FRET, fluorescence resonance energy transfer; GPCR, G-protein-coupled receptor; BAPTA-AM, 1,2-bis(*o*-aminophenoxy)ethane-*N,N,N′,N′*-tetraacetic acid tetra(acetoxymethyl) ester; eNOS, endothelial nitric-oxide synthase; DKAR, D kinase activity reporter; PI, phosphatidylinositol; PLC, phospholipase C; PDBu, phorbol-12,13-dibutyrate; PAP, phosphatidic acid phosphatase; SMS, sphingomyelin synthase; CFP, cyan fluorescent protein; YFP, yellow fluorescent protein; IP_3, inositol trisphosphate.

YFP-C1b-Y123W DNA and 0.1 μg of MyrPalm-CFP or Golgi-CFP was carried out using jetPRIME (Polyplus-transfection). Cells were imaged within 24 h following transfection.

Cell Imaging and Analysis—Cells were washed once in Hanks' balanced salt solution (cellgro) containing 1 mM CaCl₂ prior to imaging in the dark at room temperature. For Ca²⁺-buffering experiments, cells were pretreated with 15 μM BAPTA-AM for 15 min at room temperature and stimulated with 100 μM UTP followed by 200 nM PDBu. In these experiments, the FRET ratio for each cell is plotted as a percentage of the maximal response obtained following the addition of PDBu; this controls for cell-to-cell variability in the relative expression levels of FRET donor and acceptor. In phosphatidylinositol-specific phospholipase C (PI-PLC) inhibition experiments, cells were pretreated with 10 μM edelfosine for 30 min at 37 °C and then stimulated with 5 μM thapsigargin. CFP, YFP, and FRET images were acquired and analyzed as described previously (15). In Golgi-DKAR experiments without Ca²⁺, cells were incubated for 10 min in Ca²⁺-free saline and then imaged in Ca²⁺-free saline in the presence of 5 mM EGTA. Half-times ($t_{1/2}$) for Golgi DAG production were determined by fitting the data from the point of stimulation using the Exponential Rise function in Kaleida-Graph (Synergy software). Data prior to stimulation were fit with the Linear function in KaleidaGraph.

RESULTS AND DISCUSSION

Increasing Intracellular Ca²⁺ Is Sufficient to Increase DAG Levels at the Golgi—Previously, we demonstrated that increasing intracellular Ca²⁺ by treating cells with thapsigargin causes a rapid increase in plasma membrane DAG production (5). Because we have also shown that the Golgi serves as a platform for robust PKC and PKD activation following agonist stimulation (6),[3] we asked whether Ca²⁺ is the mediator that stimulates DAG production at Golgi membranes, too. To specifically monitor Golgi DAG levels, we utilized a FRET-based system consisting of a Golgi-localized FRET donor (CFP) and a DAG-binding domain (C1b domain of PKCβII harboring the Y123W mutation (11)) tagged with a FRET acceptor (YFP). The FRET donor CFP is targeted to the Golgi through the addition of a 35-amino acid targeting sequence from eNOS that localizes it to Golgi membranes (6, 14). Note that we used the C1b domain harboring the Y123W mutation because this construct has 2 orders of magnitude higher affinity for DAG than the wild-type domain (11). Generation of DAG within the membrane recruits the YFP-C1b-Y123W domain, bringing it in proximity to the FRET donor CFP, thereby resulting in an increase in FRET. By targeting the FRET donor to Golgi membranes, increases in DAG specifically at the Golgi result in an increase in the FRET ratio (Fig. 1*A*).

To determine whether Ca²⁺ is the mediator driving DAG production at the Golgi, we tested whether increasing intracellular Ca²⁺ levels was sufficient to increase Golgi DAG. Intracellular Ca²⁺ was raised by treating cells with thapsigargin, an inhibitor of the sarco/endoplasmic reticulum Ca²⁺-ATPase that causes depletion of the intracellular Ca²⁺ stores. Fig. 1*B* shows that thapsigargin treatment of COS-7 cells co-expressing

---

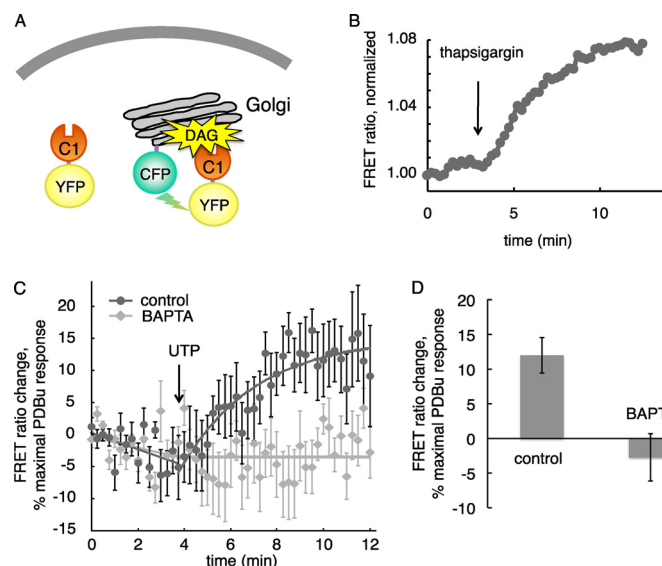[3] M. T. Kunkel and A. C. Newton, unpublished data.

FIGURE 1. **Ca²⁺ is necessary and sufficient to induce diacylglycerol production at the Golgi.** *A*, schematic representation of the Golgi DAG reporter used. A Golgi-targeted CFP and a YFP-tagged DAG-binding domain (*C1*) are co-expressed in cells. Upon production of DAG, the YFP-tagged C1 domain will translocate to membranes. An increase in FRET reflects an increase in DAG at the Golgi. *B*, COS-7 cells co-expressing a Golgi-targeted CFP and a YFP-tagged DAG-binding domain were stimulated with 5 μM thapsigargin, and the ratio of yellow emission to cyan emission was monitored over time. *C*, COS-7 cells co-expressing Golgi-targeted CFP and YFP-tagged DAG-binding domains with (*diamonds*) or without (*circles*) pretreatment with 15 μM BAPTA were stimulated with 100 μM UTP, and the ratio of yellow emission to cyan emission was monitored with time. Data are plotted as the percentage of the maximal FRET ratio change observed following 200 nM PDBu treatment. *Error bars* indicate ± S.E. *D*, bar graph depicting the average ± S.D. of the percentage of the maximal FRET ratio change in the final 2 min from the graph in *C*. Data were acquired from 23 different cells in five separate experiments. Data from time 0 to the point of UTP addition were fit to a straight line; data from the point of UTP addition were fit to a monoexponential curve.

Golgi-CFP and YFP-C1b-Y123W resulted in a pronounced increase in FRET reflecting increases in DAG at the Golgi. The addition of the phorbol ester, PDBu, to maximally recruit the reporter to membranes revealed that thapsigargin caused 50% maximal membrane binding of the reporter (data not shown). This Ca²⁺-dependent increase in DAG at Golgi membranes occurred with an ~6-fold slower rate than that previously observed at plasma membranes ($t_{1/2}$ = 4.6 min as compared with $t_{1/2}$ = 0.8 min, respectively) (5,) suggesting a distinct Ca²⁺-driven mechanism of DAG production at the Golgi as compared with plasma membrane. Furthermore, the Ca²⁺ released from intracellular stores following thapsigargin treatment was sufficient to increase Golgi DAG; removal of extracellular Ca²⁺, abolishing Ca²⁺ influx across the plasma membrane, yielded the same FRET response (data not shown). These results reveal that increasing intracellular Ca²⁺ from internal stores is sufficient to elevate Golgi DAG levels.

Ca²⁺ Is Necessary to Increase DAG Levels at the Golgi—Having established that Ca²⁺ is sufficient to induce an increase in Golgi DAG levels, we next asked whether Ca²⁺ is required for agonist-evoked increases in Golgi DAG. To this end, we examined the effect of buffering intracellular Ca²⁺ on the ability of UTP to cause Golgi DAG levels to increase. UTP treatment of COS-7 cells activates phospholipase C-coupled P2Y receptors (6) leading to the hydrolysis of phosphatidylinositol 4,5-bisphosphate to form plasma membrane DAG and inositol

trisphosphate (IP_3), which in turn leads to the release of Ca^{2+} from intracellular stores. Fig. 1*C* (*circles*) shows that UTP treatment of COS-7 cells co-expressing Golgi-CFP and YFP-C1b-Y123W resulted in an increase in FRET, indicating UTP-triggered generation of DAG at the Golgi. The increase in FRET was relatively small; normalization of the FRET change to the maximal response triggered by the subsequent addition of PDBu (which corrects for cell-to-cell variability in CFP and YFP expression) revealed that UTP caused an increase in the FRET ratio that was ~15% of the maximal amount and thus 30% of the FRET change triggered by thapsigargin treatment. Importantly, this increase was abolished in cells treated with the Ca^{2+}-chelating agent, BAPTA, which buffers Ca^{2+} levels within the cell. Indeed, no increase in the FRET ratio was observed in COS-7 cells preincubated with BAPTA (Fig. 1*C*, *diamonds*). Quantification of the maximal FRET ratio change measured (average of final 2 min of data ± S.E. from Fig. 1*C*) from five separate experiments reveals that UTP caused a 12 ± 3% increase in Golgi DAG that was abolished in BAPTA-treated cells (Fig. 1*D*). Thus, Ca^{2+} is required for DAG production at the Golgi downstream of plasma membrane GPCR activation. Interestingly, the magnitude of the FRET increase was substantially lower with UTP (12% of maximal (Fig. 1*C*)) than with thapsigargin (50% of maximal), yet the rate of Golgi DAG accumulation downstream of both of these stimuli was similar ($t_{1/2} = 4.5 \pm 0.5$ min for thapsigargin as compared with $t_{1/2} = 2.3 \pm 0.7$ min for UTP). If an additional signaling component downstream of GPCR signaling were also involved, one might predict that it would synergize with Ca^{2+} such that the rate of Golgi DAG production would be significantly faster following UTP stimulation as compared with that observed by simply elevating intracellular Ca^{2+}. Because this is not observed, it suggests that Ca^{2+} is the primary molecule driving agonist-evoked DAG increases at the Golgi.

Inhibition of PI-PLC Slows Agonist-evoked Accumulation of Plasma Membrane DAG but Not Golgi DAG—We have previously shown that inhibition of PI-PLC activities by edelfosine hinders Ca^{2+}-evoked production of DAG in plasma membranes (5). To determine whether the same family of enzymes plays a primary role in increasing Golgi DAG downstream of Ca^{2+}, COS-7 cells were preincubated with the PI-PLC inhibitor edelfosine, and Golgi DAG production was monitored by FRET. As shown in Fig. 2*A*, edelfosine slowed the rate of plasma membrane DAG accumulation over 3-fold as compared with untreated cells ($t_{1/2} = 1.43 \pm 0.03$ min as compared with $t_{1/2} = 0.43 \pm 0.03$ min, respectively). Note that data are presented as the percentage of the maximal FRET change observed following thapsigargin treatment. In comparison, the rate of Golgi DAG production was not significantly different between control cells and edelfosine-treated cells (Fig. 2*B*, $t_{1/2} = 4.5 \pm 0.5$ and 3.0 ± 0.2 min, respectively). The insensitivity of Golgi DAG production to edelfosine and the sensitivity of plasma membrane DAG production to this compound rule out PI-PLCs as the Ca^{2+} target at Golgi membranes and confirm their well described role in generating DAG at the plasma membrane.
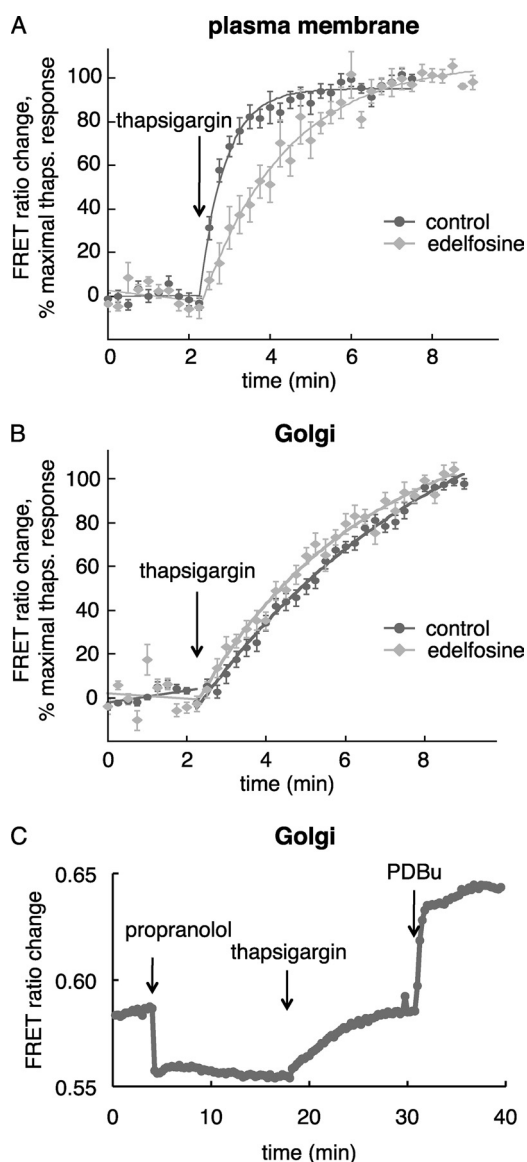

FIGURE 2. **Inhibition of phosphatidylinositol-specific phospholipase C or phosphatidic acid phosphatase does not affect the rate of diacylglycerol accumulation at Golgi.** COS-7 cells co-expressing plasma membrane-targeted CFP (*A*) or Golgi-targeted CFP (*B*) and a YFP-tagged DAG-binding domain with (*diamonds*) or without (*circles*) pretreatment with 10 μM edelfosine, to inhibit PI-PLC, were stimulated with 5 μM thapsigargin, and the ratio of yellow emission to cyan emission was monitored with time. Data from time 0 to the point of thapsigargin addition were fit to a straight line; data from the point of thapsigargin addition were fit to a monoexponential curve. *Error bars* indicate ± S.E. *C*, COS-7 cells co-expressing Golgi-targeted CFP and a YFP-tagged DAG-binding domain were treated with 500 μM propranolol, to inhibit PAP, followed by 5 μM thapsigargin and then 200 nM PDBu, and the ratio of yellow emission to cyan emission was monitored with time. Shown is a representative response from four independent experiments.

Inhibition of PAP Reduces Golgi DAG but Does Not Affect Agonist-evoked Increases in DAG—The large pool of DAG at Golgi membranes is in constant flux, and it has long been proposed that this lipid, which plays a pivotal role as second messenger in the plasma membrane, could also play a signaling role at the Golgi (16, 17). PAP and SMS contribute to the homeostasis of Golgi DAG levels; treatment of cells with the PAP inhibitor propranolol rapidly reduces the pool of DAG at Golgi membranes (12, 18), and reduction of SMS, primarily SMS1,
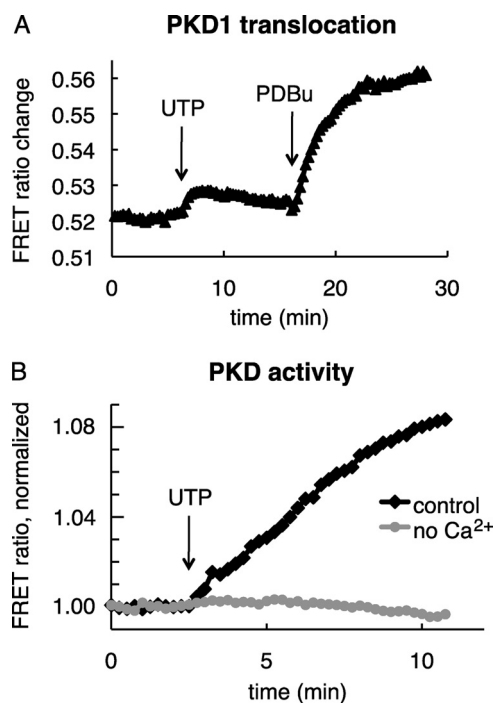
A PKD1 translocation

B PKD activity

FIGURE 3. **PKD translocates to, and signals at, the Golgi following UTP stimulation.** *A*, COS-7 cells co-expressing a Golgi-targeted CFP and a YFP-tagged PKD1 were stimulated with 100 μM UTP followed by 200 nM PDBu, and the ratio of yellow emission to cyan emission was monitored over time. Shown is a representative response from three independent experiments. *B*, COS-7 cells expressing Golgi-DKAR were stimulated with 100 μM UTP in the presence (*black diamonds*) or absence (*gray circles*) of Ca²⁺, and the ratio of cyan emission to yellow emission was monitored over time. Shown are the normalized average responses from two independent experiments.

also results in the reduction of Golgi DAG (as assessed by a reduction in localization of fluorescently tagged DAG-binding proteins). To investigate whether PAP mediates the Ca²⁺-induced increase in the Golgi DAG pool, we treated cells with the PAP inhibitor propranolol while monitoring Golgi DAG levels. As reported previously (12, 18), propranolol resulted in a marked reduction in Golgi DAG as reflected by a rapid decrease in FRET (Fig. 2*C*); the redistribution of the YFP signal from Golgi membranes to the cytosol was readily visualized (data not shown). However, following PAP inhibition, treatment of cells with thapsigargin continued to cause an increase in FRET, with the magnitude of the increase comparable with that previously observed. These results suggest that PAP is not the enzyme responding to Ca²⁺ changes and contributing to the increase in Golgi DAG. Thus, although the nature of the enzyme machinery that produces agonist-evoked DAG at the Golgi remains to be elucidated, it is neither a PI-PLC nor a PAP.

The Golgi Is a Platform for PKD Activity—Having identified a role for Ca²⁺ in increasing Golgi DAG levels downstream of plasma membrane signals, we next examined whether this increase could induce translocation of the C1 domain-containing kinase PKD1 to the Golgi. To assess this, we monitored FRET changes between Golgi-CFP and a YFP-tagged PKD1. As shown in Fig. 3*A*, PKD1 translocated to Golgi membranes following UTP treatment. Thus, the DAG generated at the Golgi following UTP stimulation of cells was sufficient to increase the binding of PKD.
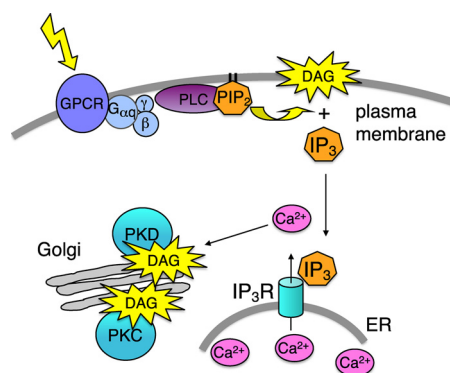

FIGURE 4. **Model illustrating Ca²⁺ as the second messenger that transduces plasma membrane GPCR signals to produce diacylglycerol at the Golgi.** Stimulation of Gα_q-coupled receptors leads to G-protein-mediated activation of PLC to catalyze the hydrolysis of phosphatidylinositol bisphosphate (*PIP₂*) to generate DAG and IP₃. IP₃ binds the IP₃ receptor (*IP₃R*) on endoplasmic reticulum (*ER*) membranes, triggering the release of Ca²⁺ from intracellular stores. This increase in cellular Ca²⁺ is both necessary and sufficient to induce an increase in Golgi membrane DAG levels. Increases in DAG at the Golgi allow it to serve as a platform for agonist-evoked recruitment and activation of PKC and PKD.

To address whether binding to Golgi membrane resulted in activation of PKD, we monitored the activity of PKD using a Golgi-targeted PKD activity reporter (Golgi-DKAR). DKAR is a genetically encoded, PKD-specific, kinase activity reporter consisting of a FRET pair that flanks a phosphoamino acid-binding domain and a PKD consensus sequence (5). Activated PKD phosphorylates DKAR, inducing a conformational change that results in a change in intramolecular FRET. One can monitor localized PKD activity by poising DKAR at distinct subcellular regions; thus, Golgi-DKAR was targeted to Golgi membranes via fusion of the N-terminal residues of eNOS as had been done to target CFP above. Fig. 3*B* reveals that UTP stimulation induced an increase in PKD activity as assessed by a change in the FRET ratio of Golgi-DKAR. To determine the contribution of intracellular Ca²⁺ on PKD activity at the Golgi, we monitored Golgi-DKAR FRET under conditions in which intracellular Ca²⁺ levels would not change; by preincubating cells in Ca²⁺-free saline and imaging in the presence of EGTA, intracellular Ca²⁺ levels do not increase following GPCR activation. Under these conditions, there was no change in FRET from Golgi-DKAR, indicating the requirement of Ca²⁺ for induction of PKD activity at Golgi membranes (Fig. 3*B*). A similar result was observed when monitoring PKC activity under these same conditions (6). Importantly, Golgi-DKAR still displayed a change in FRET following the addition of PDBu, indicating that PKD was still competent to signal under these conditions (data not shown). Thus, Ca²⁺ is necessary for the activation of two DAG-controlled kinases, PKD and PKC, at the Golgi.

Conclusion—Here we identify Ca²⁺ as the second messenger that links signals received at the plasma membrane to lipid hydrolysis at the Golgi. Specifically, we show that elevations in intracellular Ca²⁺ attendant to GPCR activation signal the production of DAG at Golgi membranes. As illustrated in Fig. 4, stimulation of G$_q$-coupled receptors leads to the PLC-catalyzed hydrolysis of phosphatidylinositol bisphosphate (*PIP₂*) to form

two second messengers, plasma membrane DAG and IP_3. IP_3 binds the IP_3 receptor on endoplasmic reticulum (*ER*) membranes, thus stimulating the release of Ca^{2+} into the cytosol, an event that, in turn, signals DAG accumulation at Golgi membranes. This allows the Golgi to coordinate the binding and activation of DAG-controlled kinases such as PKC and PKD, two kinases that are robustly activated at the Golgi in response to signals received at the plasma membrane (6).

REFERENCES

1. Yang, C., and Kazanietz, M. G. (2003) *Trends Pharmacol. Sci.* **24,** 602–608
2. Toker, A. (2005) *EMBO Rep.* **6,** 310–314
3. Griner, E. M., and Kazanietz, M. G. (2007) *Nat. Rev. Cancer* **7,** 281–294
4. Violin, J. D., Zhang, J., Tsien, R. Y., and Newton, A. C. (2003) *J. Cell Biol.* **161,** 899–909
5. Kunkel, M. T., Toker, A., Tsien, R. Y., and Newton, A. C. (2007) *J. Biol. Chem.* **282,** 6733–6742
6. Gallegos, L. L., Kunkel, M. T., and Newton, A. C. (2006) *J. Biol. Chem.* **281,** 30947–30956
7. Bossard, C., Bresson, D., Polishchuk, R. S., and Malhotra, V. (2007) *J. Cell Biol.* **179,** 1123–1131
8. Ghanekar, Y., and Lowe, M. (2005) *Trends Cell Biol.* **15,** 511–514
9. Hausser, A., Storz, P., Märtens, S., Link, G., Toker, A., and Pfizenmaier, K. (2005) *Nat. Cell Biol.* **7,** 880–886
10. Maeda, Y., Beznoussenko, G. V., Van Lint, J., Mironov, A. A., and Malhotra, V. (2001) *EMBO J.* **20,** 5982–5990
11. Dries, D. R., Gallegos, L. L., and Newton, A. C. (2007) *J. Biol. Chem.* **282,** 826–830
12. Baron, C. L., and Malhotra, V. (2002) *Science* **295,** 325–328
13. Villani, M., Subathra, M., Im, Y. B., Choi, Y., Signorelli, P., Del Poeta, M., and Luberto, C. (2008) *Biochem. J.* **414,** 31–41
14. Liu, J., Hughes, T. E., and Sessa, W. C. (1997) *J. Cell Biol.* **137,** 1525–1535
15. Kunkel, M. T., Ni, Q., Tsien, R. Y., Zhang, J., and Newton, A. C. (2005) *J. Biol. Chem.* **280,** 5581–5587
16. Pagano, R. E. (1988) *Trends Biochem. Sci.* **13,** 202–205
17. van Meer, G. (1998) *Trends Cell Biol.* **8,** 29–33
18. Fernández-Ulibarri, I., Vilella, M., Lázaro-Diéguez, F., Sarri, E., Martínez, S. E., Jiménez, N., Claro, E., Mérida, I., Burger, K. N., and Egea, G. (2007) *Mol. Biol. Cell* **18,** 3250–3263